# Chapter 2: An Intersubunit Hydrogen Bond in the Nicotinic Acetylcholine Receptor that Contributes to Channel Gating

This research was originally published in Journal of Biological Chemistry. Kristin Rule Gleitsman, Sean M. A. Kedrowski, Henry A. Lester, Dennis A. Dougherty J. Biol. Chem. **2008**, *283*, 35638-35643. 

## 2.1 Abstract

The muscle nicotinic acetylcholine receptor (nAChR) is a large, allosteric, ligand-gated ion channel with the subunit composition $\alpha_2\beta\gamma\delta$. Though much is now known about the structure of the binding site, relatively little is understood about how the binding event is communicated to the channel gate, causing the pore to open. Here we identify a key hydrogen bond near the binding site that is involved in the gating pathway. Using mutant cycle analysis with the novel unnatural residue α-hydroxyserine (Sah), we find that the backbone N-H of αS191 in loop C makes a hydrogen bond to an anionic side chain of the complementary subunit upon agonist binding. However, the anionic partner is not the glutamate predicted by the crystal structures of the homologous acetylcholine binding protein (AChBP). Instead, the hydrogen bonding partner is the extensively researched aspartate γD174/δD180—which had originally been identified as a key binding residue for cationic agonists.

## 2.2 Introduction

The Cys-loop family of ligand-gated ion channels is involved in mediating fast synaptic transmission throughout the central and peripheral nervous systems{Corringer, 2000 #8; Grutter, 2001 #10; Karlin, 2002 #11}. These neuroreceptors are among the molecules of learning, memory, and sensory perception, and they are implicated in numerous neurological disorders, including Alzheimer's disease, Parkinson's disease, and schizophrenia. The muscle nicotinic acetylcholine receptor (nAChR) is arguably the best-studied member of the Cys-loop family. This heteropentameric receptor is composed of homologous, but functionally distinct, subunits

arranged symmetrically around a central ion-conducting pore with the stoichiometry $\alpha_2\beta\gamma\delta$. The agonist binding sites are located at the interfaces between the αγ and αδ subunits. The binding of two agonist molecules induces a conformational change that leads to the opening of the ion channel.

It is now widely appreciated that a tryptophan residue (αW149) plays a key role in neurotransmitter binding by forming a cation-π interaction with the quaternary ammonium group of acetylcholine{Zhong, 1998 #15}, a result supported by structural data. However, many other important residues in the immediate vicinity of the binding site have been identified. In a classic experiment on the *Torpedo* nAChR (a close homologue of the muscle subtype), Czajkowski and Karlin concluded that a key aspartate (γD174/δD180) from the complementary binding subunit could come within 9 Å of the agonist binding site{Czajkowski, 1991 #1}. Mutation of this residue severely impacted receptor function, leading to a proposal that the negative charge of this aspartate interacted with the positive charge of the agonist{Czajkowski, 1995 #2; Czajkowski, 1993 #3}. Subsequently, however, both the crystal structure of acetylcholine-binding protein (AChBP, a soluble protein homologous to the extracellular domain of the nAChR){Brejc, 2001 #16} and the 4 Å cryo-EM structure of *Torpedo* nAChR{Miyazawa, 1999 #12; Unwin, 2005 #36} showed that this residue is positioned quite far from the agonist binding site (Figure 2.1). Single-channel studies suggest that this residue is primarily important for ligand-induced channel gating rather than agonist binding{Akk, 1999 #14; Sine, 2002 #13}.

γD174/δD180 is part of loop F, the most remote of the six loops originally proposed by Changeux to contribute to the agonist binding site{Corringer, 2000 #8}. In the carbamylcholine-bound AChBP structure{Sixma, 2003 #32}, a different F loop anionic residue, γE176/δE182 (AChBP E163), is positioned near loop C of the agonist binding site (Figure 2.1). Specifically,

γE176/δE182 is within hydrogen bonding distance of the backbone N-H at αS191, which is located on the C loop between the aromatic binding box residue αY190 and the vicinal disulfide formed by αC192 and αC193. Loop F is generally disordered in the AChBP and nAChR structures, and hydrogen-deuterium exchange mass spectrometry on AChBP reveals that loop F and loop C are the most conformationally dynamic segments of the protein{Shi, 2006 #6}. It is generally accepted that agonist binding draws loop C inward, capping the aromatic binding pocket{Hansen, 2005 #7; Sixma, 2003 #32}. In contrast, crystal structures of AChBP with antagonists bound reveal loop C pulled away from the agonist binding site{Hansen, 2005 #7}. Distinctions between antagonist- and agonist-induced motion have also been observed in loop F{Hibbs, 2006 #33}. As such, many investigators favor a gating model involving a contraction of the agonist binding site around an agonist molecule that is largely mediated by movements in loops C and F, though little is known about the nature of the specific interactions involved in this systolic motion.

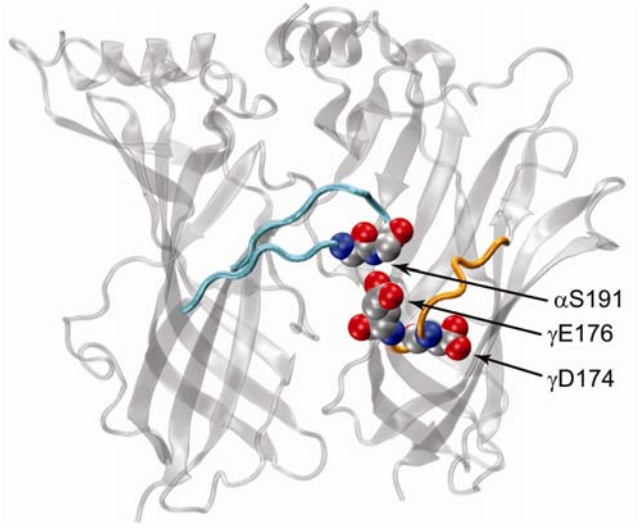


**Figure 2.1. Structure of AChBP with carbamylcholine bound (pdb: 1UV6); numbering as in nAChR. Residues considered here are shown in space-filling. The C loop (cyan) and F loop (orange) are highlighted. In this structure, the C and F loops have closed around the bound agonist (agonist not shown). A carboxylate oxygen (red) of γE176 is within hydrogen bonding distance of the backbone NH (blue) of αS191.**

In the present work we evaluate several anionic residues in loop F and potential interactions with loop C. Using a combination of natural and unnatural mutagenesis, we find that, indeed, the backbone N-H of αS191 does make a hydrogen bond to a loop F residue.

However, the partner is not the glutamate seen in the AChBP crystal structure. Instead, the aspartate (γD174/δD180) originally identified by Czajkowski and Karlin is the hydrogen bonding partner.

**2.3 Results**

*A Backbone Mutation at αS191 Has a Large Impact on Receptor Function*

In the process of probing the backbone flexibility surrounding the nAChR binding box, we mutated αS191 to α-hydroxyserine (Sah). This produces an ester backbone linkage at this position, while preserving the side chain. Along with increasing backbone flexibility, this mutation removes the hydrogen bond-donating N-H group and replaces it with a non-hydrogen bond-donating O (Figure 2.2, 2.3). We have performed similar backbone mutations at several positions throughout the nAChR, and typically the consequences are not dramatic{England, 1999 #31; Cashin, 2007 #17}. However, at αS191, this subtle mutation leads to a 40-fold increase in $EC_{50}$ (Table 2.1 & Figure 2.2b). We also made alanine and α-hydroxyalanine (Aah) mutations at this site. The side chain mutation alone had minimal impact on receptor function, producing no shift in $EC_{50}$. However, receptor function of the αS191Aah mutant was dramatically impaired relative to αS191Ala, confirming that the backbone—and not the side chain—at αS191 is important for receptor function.

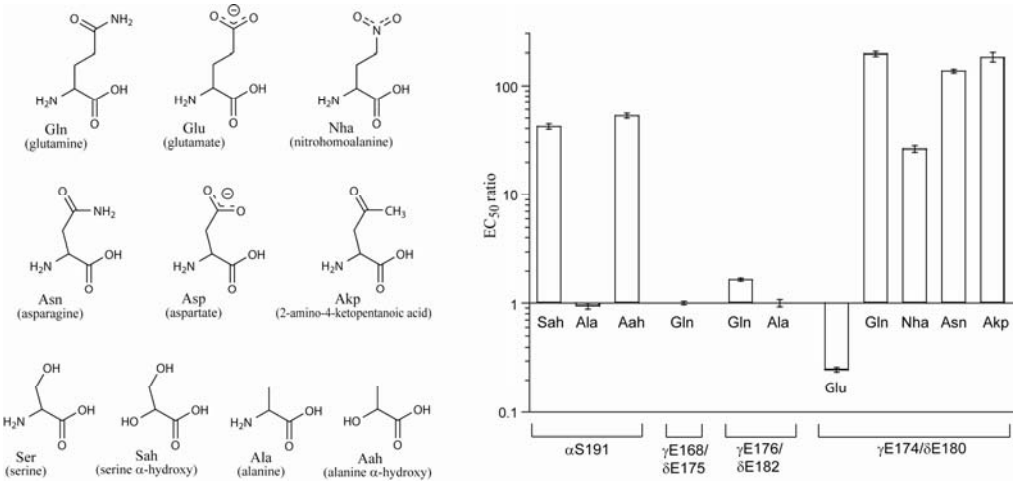


**Figure 2.2 (A) Natural and unnatural residues used in this study. (B) $EC_{50}$ ratios (mutant/wild type) for natural and unnatural substitutions at four sites in the extracellular domain. For glutamine and Nha, $EC_{50}$ ratios were calculated with reference to glutamate instead of wild type (aspartate).**

| Mutant | $EC_{50}$ (μM) | Double Mutant | $EC_{50}$ (μM) | ΔΔG (kcal/mol) |
|---|---|---|---|---|
| αβγδ | 1.2 ± 0.04 | | | |
| αS191βγδ Sah | 50 ± 2.3 | | | |
| αβγE176AδE182A | 1.2 ± 0.08 | αS191SahβγE176AδE182A | 32 ± 1.7 | 0.27 ± 0.06 |
| αβγE176QδE182Q | 2.0 ± 0.10 | αS191SahβγE176QδE182Q | 51 ± 2.4 | 0.29 ± 0.03 |
| αβγE168QδE175Q | 1.2 ± 0.02 | αS191SahβγE168QδE175Q | 37 ± 1.2 | 0.18 ± 0.05 |
| αβγD174EδD180E | 0.3 ± 0.01 | αS191SahβγD174EδD180E | 15 ± 0.90 | 0.12 ± 0.05 |
| αβγD174QδD180Q | 59 ± 2.0 | αS191SahβγD174QδD180Q | 96 ± 5.2 | 1.9 ± 0.05 |
| αβγD174NhaδD180Nha | 7.9 ± 0.40 | αS191SahβγD174NhaδD180Nha | 31 ± 1.9 | 1.4 ± 0.05 |
| αβγD174NδD180N | 160 ± 2.7 | αS191SahβγD174NδD180N | 190 ± 12 | 2.1 ± 0.05 |
| αβγD174AkpδD180Akp | 220 ± 19 | αS191SahβγD174AkpδD180Akp | 190 ± 12 | 2.3 ± 0.15 |
| αS191βγδ Ala | 1.1 ± 0.06 | αS191AlaβγD174NδD180N | 230 ± 8.0 | 0.25 ± 0.04 |
| αS191βγδ Aah | 63 ± 2.4 | αS191AahβγD174NδD180N | 130 ± 7.6 | 2.5 ± 0.04 |

**Table 2.1. $EC_{50}$ values ± the standard error of the mean for mutations made in this study. In all cases the β-subunit contains a L9'S mutation.**

*Evaluating anionic residues on loop F*

To evaluate the potential hydrogen bond from αS191 to γE176/δE182, we made several mutations at this glutamate. Surprisingly, all mutations have minimal impact, suggesting no critical role for this residue. Another nearby loop F glutamate residue, γE169/δE175, was also evaluated. Again, no significant impact is seen.

In sharp contrast, even the subtlest mutations at γD174/δD180 produce large effects on receptor function, a result that others have also seen{Czajkowski, 1991 #1; Czajkowski, 1995 #2; Martin, 1996 #5; Martin, 1997 #4}. We first studied asparagine, glutamate and glutamine mutations at this site. The γD174E/δD180E mutant exhibits a modest ~3-fold decrease in $EC_{50}$. However, the γD174N/δD180N and γD174Q/δD180Q mutants produce substantial (>100-fold) changes to the $EC_{50}$ (Figure 2.2b and Table 2.1).

Fundamentally, the results of these conventional mutations strongly implicate the side chain of γD174/δD180 in an electrostatic interaction, such as an ion pair or hydrogen bond. However, changing the side chain functionality from a carboxylate to an amide not only neutralizes the charge on the side chain, it also desymmetrizes it and introduces a potential hydrogen bond donor. To better understand the role of γD174/δD180, we incorporated two unnatural amino acids.

Nitrohomoalanine (Nha) is an analogue of glutamate that contains a nitro ($NO_2$) group, which is isosteric and isoelectronic to a carboxylate, but it has no charge and is a much weaker hydrogen bond acceptor (Figure 2.2a).[*] Incorporation of Nha at γD174/δD180 yields a slightly less dramatic effect than the γD174N/δD180N and γD174Q/δD180Q mutants, producing a 24-

[*] Although nitroalanine, the analogue of aspartate, would be ideal, it is not chemically compatible with the nonsense suppression methodology. Given that the mutation γD174E/δD180E produces a very modest $EC_{50}$ shift and that γD174N/δD180N and γD174Q/δD180Q show similar effects on receptor function, the comparison of Nha to Glu can be considered meaningful.

fold shift in $EC_{50}$ relative to γD174E/δD180E (Figure 2.2b). Thus, charge neutralization at this site significantly affects receptor function but cannot fully account for the $EC_{50}$ shift seen in the γD174N/δD180N and γD174Q/δD180Q mutants.

The second unnatural amino acid analogue incorporated at γD174/δD180 was 2-amino-4-ketopentanoic acid (Akp). Akp is isoelectronic to Asp, but possesses a methyl ketone functionality in place of the carboxylate (Figure 2.2a). As such, Akp is a desymmetrized analogue of Asp—similar to Asn—but it has different electrostatic properties (less polar, weaker hydrogen bond acceptor, and cannot donate a hydrogen bond). When Akp is incorporated at γD174/δD180, its effect upon receptor function is roughly as deleterious as the Asn mutation (Figure 2.2b).

Mutations at individual binding sites (αβγD174Nδ and αβγδD180N) showed substantial (~50-fold) and approximately equivalent increases in whole cell $EC_{50}$.

*Mutant cycle analysis reveals a strong interaction between the αS191 backbone and the side chain of γD174/δD180*

Mutant cycle analysis was performed between several of the side chain mutations at γD174/δD180 and the αS191Sah mutation (Figure 2.3, 2.4). Briefly, mutant cycle analysis is used to determine the pairwise interaction energy between two residues in a protein using the equation given in Figure 2.3. If the two residues do not interact, the change in free energy for the simultaneous mutation of both residues should simply be the sum of the free energy of each of the individual mutations. However, for residues that interact, the change in free energy for the double mutation will be non-additive. $EC_{50}$-based mutant cycle analysis has been used to

investigate interactions in Cys-loop receptors by other researchers{Kash, 2003 #18; Price, 2007 #19; Venkatachalan, 2008 #20}.

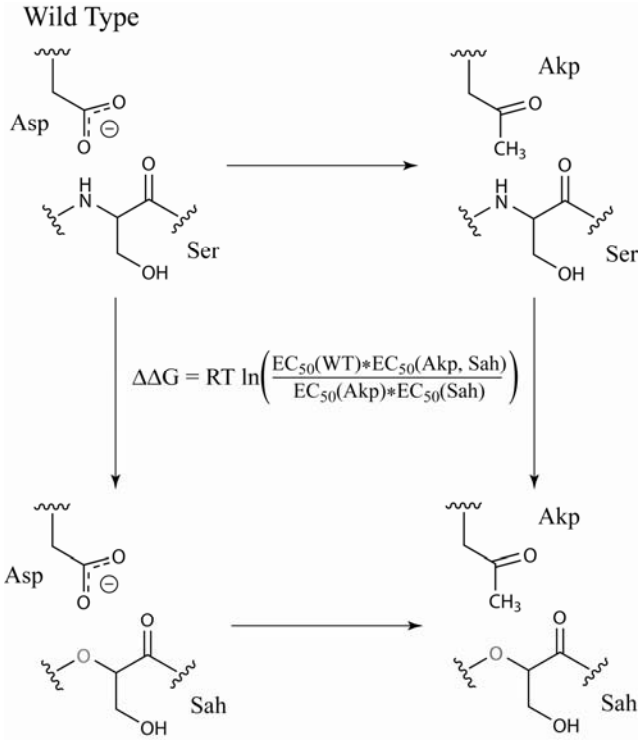


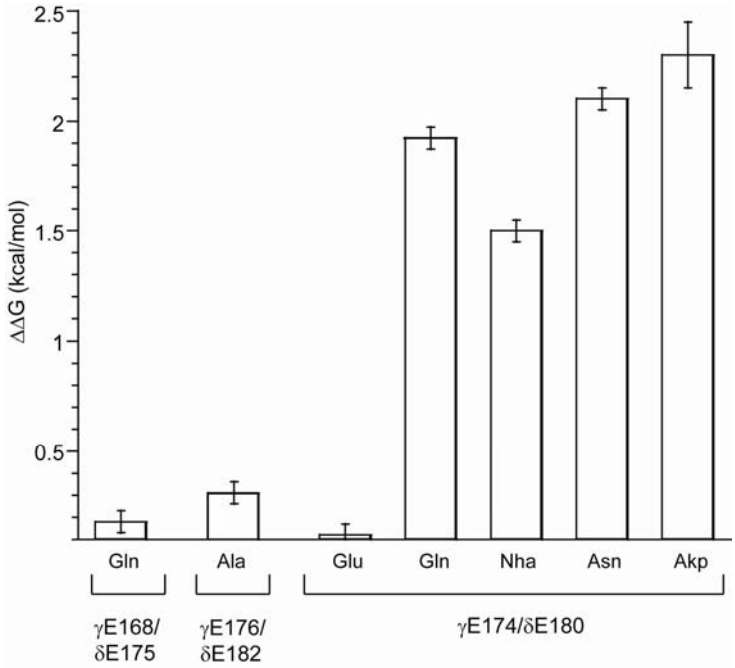


**Figure 2.4: Coupling energies between various side chain mutants in the complementary binding subunit and the backbone mutation at αS191 (αS191Sah). For glutamine and Nha, free energy calculations were made with reference to glutamate instead of wild type (aspartate).**

Lengthening the side chain (γD174E/δD180E) has no impact on the interaction between these two residues (ΔΔG = 0.12 kcal/mol). In contrast, mutant cycle analysis between γD174N/δD180N and αS191Sah indicates a large energetic coupling (ΔΔG = 2.1 kcal/mol). A smaller but still quite significant effect is seen for the mutant cycle analysis between γD174Nha/δD180Nha and αS191Sah (ΔΔG = 1.4 kcal/mol). Mutant cycle analyses of γD174N/δD180N with αS191A and αS191Aah further support the conclusion that the interaction between these residues involves the backbone of αS191 and not the side chain (αS191Ala: ΔΔG = 0.25; αS191Aah: ΔΔG = 2.3 kcal/mol). Not surprisingly, comparable mutant cycle analyses of the two glutamates of loop F, γE176/δE182 and γE169/δE175, with αS191Sah showed no significant coupling.

**2.4 Discussion**

The AChBP crystal structures transformed the study of nAChRs by providing high resolution structural data about the ligand binding domain of these proteins. In addition to refining our existing structural knowledge of the receptor—obtained from decades of careful biochemical research—it served as a valuable starting point for new structure-function studies on the receptor. However, AChBP is not a ligand-gated ion channel and, in fact, shares less than 25% homology with its nearest Cys-loop relative, the α7 nAChR{Brejc, 2001 #16}. As such, some fundamental structural differences must exist between AChBP and actual Cys-loop receptors, particularly pertaining to residues involved in mediating communication between the binding site and the ion channel pore.

Arguably the biggest discrepancy between the AChBP structures and prior biochemical studies of the nAChR concerns the loop F residue γD174/δD180. A remarkable cross-linking study in the *Torpedo* nAChR indicated that this residue can come within 9 Å of the vicinal

disulfide on the C loop, located at the heart of the agonist binding site{Czajkowski, 1991 #1}. Yet, in AChBP the residue that aligns with γD174/δD180 is not at all near the agonist binding site. In addition, the cryo-EM structure of the *Torpedo* nAChR, which is believed to be in the desensitized or closed state, places this residue tucked deeply inside a β-sheet-lined hydrophobic pocket, over 15 Å from loop C{Miyazawa, 1999 #12; Unwin, 2005 #36}.

While γD174/δD180 is remote to the agonist binding site in AChBP, another loop F anionic residue, γE176/δE182, appears to make a hydrogen bond to a backbone N-H that is integral to the aromatic box of the agonist binding site when the agonist carbamylcholine is bound. Using nonsense suppression methodology, we have been able to specifically remove the backbone N-H in question by replacing αS191 with its α-hydroxy analogue. Consistent with the AChBP images, this subtle structural change has a large effect on receptor function, suggesting that a hydrogen bond to this moiety is important. However, consistent with prior mutational analyses{Czajkowski, 1995 #2; Czajkowski, 1993 #3; Martin, 1996 #5}, we find that γE176/δE182 does not play a large role in receptor function. This suggests that AChBP does not provide an accurate model of the muscle nAChR in this region. Given that the sequence alignment in this region shows a number of insertions in nAChR relative to AChBP—combined with the fact that the F loop is believed to be involved in gating the nAChR (AChBP does not gate)—it is not surprising that AChBP would be an unreliable model here.

Our results indicate that the hydrogen-bonding partner for the backbone N-H of αS191 in the nAChR is instead the side chain of γD174/δD180. Based on the available structural and functional data, we suggest that this hydrogen bond exists in the open state only{Akk, 1999 #14; Martin, 1996 #5; Martin, 1997 #4}. As others have seen, a number of mutations of this side chain profoundly affect receptor function. Here we employ several relatively subtle mutations.

The fact that substantial functional consequences are seen suggests a precise structural role for this side chain in at least one state crucial for activating the channel. Furthermore, all mutations at γD174/δD180 that significantly impact function also show strong coupling to the αS191Sah backbone mutation via mutant cycle analysis. The nature of the coupling is as one would expect from the hydrogen bonding model: mutation at either site has a strong effect; however, once the αS191Sah mutation is introduced—removing any possible hydrogen bonding interaction—mutations at γD174/δD180 have a *much* smaller impact. Interestingly, no specific role for the side chain of αS191 is found, as the αS191A mutant gives essentially wild type behavior.[†] However, when the alanine side chain is combined with the α-hydroxy backbone mutation, the same coupling to γD174/δD180 is observed.

We propose that the movement of loop F of the complementary subunit from a position remote to the agonist binding site to one of close proximity to loop C of the principal subunit is a key early structural change associated with nAChR gating. Driving this structural reorganization is the formation of a hydrogen bond between the side chain of γD174/δD180 and the backbone N-H of αS191. In the closed state of the wild-type receptor, αS191 and the C loop project out into solution, away from the bulk of the receptor, while γD174/δD180 of the F loop projects deep within a hydrophobic cavity. Though the energetic desolvation penalty of burying a charged residue within a hydrophobic cavity is significant[‡], it alone is apparently not sufficient to overcome other structural elements that bias this conformation of the F loop. However, agonist binding induces a centripetal movement of the C loop, bringing the backbone N-H of αS191 in closer proximity to the F loop. This structural change makes possible a hydrogen bond between γD174/δD180 and the C loop backbone. We hypothesize that the formation of this hydrogen

[†] In AChBP structures, the αS191 side chain also makes hydrogen bonds toγE176/δE182.

[‡] Based on the hydrophobicity constant, π, the expected desolvation penalty for an aspartic acid residue would be on the order of 1 kcal/mol ({Eisenberg, 1986 #38}

bond, along with the energetic solvation benefit of moving γD174/δD180 into an aqueous environment, provides sufficient driving force to move γD174/δD180 out of its pocket, inducing a movement of the F loop toward the C loop.[§] This structural rearrangement of loop F contributes to the gating pathway. Using rate-equilibrium free energy relationships, Auerbach and coworkers have also concluded that γD174/δD180 moves early in the gating process{Grosman, 2000 #9}.

Our results provide an explanation for the cross-linking studies of Czajkowski and Karlin{Czajkowski, 1991 #1}, and they are not in conflict with available structural information. The cryo-EM images of the *Torpedo* receptor show greater than 20 Å separation between αS191 and γD174/δD180 in the closed state. Still, the distance of less than 9 Å that is suggested by the cross-linking studies is plausible, provided that the residues are free to move closer, as occurs in our model of channel gating. A comparison of AChBP structures with and without agonist bound likewise shows that motions of loops C and F are the dominant structural rearrangements that occur when agonist binds. The fact that the hydrogen bond acceptor in loop F differs between AChBP and nAChR is not surprising, given that loop F is strongly implicated in nAChR gating and AChBP did not evolve to have a gating function.

This model is also consistent with the γD174/δD180 mutants described here. Lengthening the sidechain of this key F loop residue (γD174E/δD180E) effects a modest improvement in receptor function, either because the longer side chain can more easily reach its αS191 hydrogen bonding partner, or because it fits more poorly in the hydrophobic pocket, destabilizing the closed state. Any mutation that eliminates side chain charge has a significant

[§] The possibility of a salt bridge forming here can be eliminated, given that there are no basic residues in the C loop or in its vicinity.

impact on function, which is expected, given that these mutant side chains are poorer hydrogen bond acceptors and that they experience a much lower energetic solvation benefit upon moving from the hydrophobic pocket into an aqueous environment.

In conclusion, mutant cycle analysis involving a novel backbone mutant has identified an important interaction between an F loop residue that has long been thought to contribute to receptor function and the peptide backbone of loop C. The hydrogen bond between the side chain of γD174/δD180 and the backbone of αS191 likely forms upon agonist binding and is part of the agonist-induced conformational changes that lead to channel opening. Along with contributing new insights into the gating pathway of the nAChR, our results reconcile a long-standing discrepancy between early biochemical studies of the receptor and structural models from the AChBP systems.

**2.5 Materials and Methods**

*Preparation of Unnatural Amino and Hydroxy Acids*

All chemical reactions were performed under argon using solvent-column dry solvents{Pangborn, 1996 #22}. Flasks and vials were oven dried at 122°C and cooled in a desiccator box containing anhydrous calcium sulfate. Silica chromatography was carried out in accordance with the methods of Still{Still, 1978 #23}. The preparations of Nha, Akp, and Aah have been described previously{Cashin, 2007 #17; England, 1999 #24; Mu, 2006 #34}.

*Synthesis of 2,3-dihydroxypropionate (α-hydroxyserine, Sah)-tRNA*

Glycerate, calcium salt dihydrate (286 mg, 2.0 mmol) was measured into a 100 mL round-bottomed flask. Methanol (40 mL) and toluene (10 mL) were added, followed by conc.

hydrochloric acid (1 mL, 12 mmol). The mixture was stirred under reflux for 6 h, at which point the solvent was removed *in vacuo*. This crude residue was then dissolved in dimethylfomamide (6 mL) in a 2-dram vial. *tert*-butyldimethylsilyl chloride (906 mg, 6 mmol) and Imidazole (544 mg, 8 mmol) were then added, and the reaction was stirred at room temperature for 12 h, at which point the reaction was concentrated *in vacuo* to ca. 1 mL, and dichloromethane (10 mL) was added. The precipitate was removed by filtration, and the filtrate was reduced *in vacuo* and purified by flash chromatography on silica (5% ethyl acetate in hexanes) to yield 421 mg (60% over 2 steps) 2,3-di-*tert*-butyldimethylsilyl-glycerate methyl ester. $^{1}$H NMR (300 MHz, $CDCl_3$) $\delta$ 4.27 (dd, 1H, $J$ = 5.2, 6.2 Hz), 3.80 (dd, 1H, $J_{AB}$ = 9.9 Hz, $J_{AX}$ = 5.2 Hz), 3.73 (dd, 1H, $J_{AB}$ = 9.9 Hz, $J_{AX}$ = 6.6 Hz), 3.70 (s, 3H), 0.88 (s, 9H), 0.85 (s, 9H), 0.07 (s, 3H), 0.05 (s, 3H), 0.03 (s, 3H), 0.02 (s, 3H). $^{13}$C NMR (75 MHz, $CDCl_3$) $\delta$ 172.71, 74.21, 66.16, 51.99, 26.04, 25.94, 18.57, 18.52, -4.86, -4.87, -5.16, -5.25. LRMS ($ES^+$) calculated for [$C_{16}H_{36}NaO_4Si_2$] ([M+Na]$^+$) 371.2, found 371.1.

2,3-di-*tert*-butyldimethylsilylglycerate methyl ester (100 mg, 0.29 mmol) was measured into a 2-dram vial. Diethyl ether (3 mL) was added to dissolve the starting material, followed by potassium trimethylsilanolate{Laganis, 1984 #37} (40.7 mg, 0.29 mmol). After 18 h, the potassium salt was isolated by filtration, washed with 2 x 1 mL ether, and dried *in vacuo*. The solid was then resuspended in chloroacetonitrile (3 mL) and allowed to stir at room temperature for 6 h. The reaction was then filtered through a plug of silica to yield the pure product as a colorless liquid: 66.7 mg (62% over 2 steps) 2,3-di-*tert*-butyldimethylsilylglycerate cyanomethyl ester. $^{1}$H NMR (300 MHz, $CDCl_3$) $\delta$ 4.75 (s, 2H), 4.35 (t, 1H, $J$ = 5.4 Hz), 3.81 (d, 2H, $J$ = 5.4 Hz), 0.90 (s, 9H), 0.87 (s, 9H), 0.10 (s, 3H), 0.08 (s, 3H), 0.06 (s, 3H), 0.05 (s, 3H). $^{13}$C NMR (75 MHz, $CDCl_3$) $\delta$ 170.82, 114.24, 73.78, 65.92, 48.62, 26.01, 25.87, 18.48, -4.86, -4.90, -5.21, -5.24. HRMS ($FAB^+$) calculated for [$C_{17}H_{36}NO_4Si_2$] ([M+H]$^+$) 374.2183, found 374.2181.

The transesterification and deprotection of 2,3-di-*tert*-butyldimethylsilylglycerate cyanomethyl ester were performed according to published protocols to yield Sah-tRNA{Nowak, 1998 #35}.

*Side chain and backbone mutagenesis*

Conventional mutagenesis and unnatural mutagenesis, with the site of interest mutated to either an amber stop codon or a four base frameshift codon (at αS191), were achieved by a standard Stratagene QuikChange protocol. Sequencing through both strands confirmed the presence of the desired mutation. Mouse muscle embryonic nAChR in the pAMV vector was used. All the mutations were made in the presence of a background transmembrane mutation (βL9'S) that lowers whole-cell $EC_{50}$ {Filatov, 1995 #30; Labarca, 1995 #29}. In addition, the α-subunits contain an HA epitope in the M3-M4 cytoplasmic loop for Western blot studies. Control experiments show that this epitope does not detectably alter $EC_{50}$. mRNA was prepared by in vitro runoff transcription using the Ambion (Austin, TX) T7 mMessage mMachine kit. For conventional mutants, a total of 2.0-4.0 ng of mRNA was injected in a ratio of 2:1:1:1 of α:β:γ:δ. For suppression with unnatural amino and hydroxy acids, a total of 4.0 ng of mRNA was injected in an α:β:γ:δ subunit ratio of 10:1:1:1. Typically, 25 ng of tRNA was injected per oocyte along with mRNA in a ratio of 1:1 with a total volume of 50 nL/cell. As a negative control for suppression, truncated 74-nucleotide tRNA or truncated tRNA ligated to dCA was co injected with mRNA in the same manner as fully charged tRNA. Data from experiments where currents from these negative controls were greater than 10% of the experimental were excluded. Frameshift suppression at αS191 was used for simultaneous incorporation of two unnatural residues{Rodriguez, 2006 #26}.

*Electrophysiology*

The function of mutant receptors was evaluated using two-electrode voltage clamp. Stage V-VI oocytes of *Xenopus laevis* were employed. Oocyte recordings were made 12-48 h postinjection in two-electrode voltage clamp mode using the OpusXpress 6000A instrument (Axon Instruments, Union City, CA). Oocytes were superfused with a $Ca^{2+}$-free ND96 solution at flow rates of 1 mL/min before application, 4 mL/min during drug application, and 3 mL/min during wash. Holding potential was -60 mV. Data were sampled at 125 Hz and filtered at 50 Hz. Drug applications were 15 s in duration. Acetylcholine chloride was purchased from Sigma/Aldrich/RBI. Solutions ranging from 0.01 to 5000 µM were prepared in $Ca^{2+}$-free ND96 from a 1 M stock solution. Dose-response data were obtained for a minimum of 8 concentrations of agonists and for a minimum of five cells. Dose-response relations were fitted to the Hill equation to determine $EC_{50}$ and Hill coefficient values. The dose-response relations of individual oocytes were examined and used to determine outliers. The reported $EC_{50}$ values are from the curve fit of the averaged data.

**2.6 References**


1. Corringer, P.J., Le Novere, N. & Changeux, J.P. Nicotinic receptors at the amino acid level. Annu Rev Pharmacol Toxicol **40**, 431-58 (2000).
2. Grutter, T. & Changeux, J.P. Nicotinic receptors in wonderland. Trends Biochem Sci **26**, 459-63 (2001).
3. Karlin, A. Emerging structure of the nicotinic acetylcholine receptors. Nat Rev Neurosci **3**, 102-14 (2002).
4. Zhong, W. et al. From ab initio quantum mechanics to molecular neurobiology: a cation-pi binding site in the nicotinic receptor. Proc Natl Acad Sci U S A **95**, 12088-93 (1998).
5. Czajkowski, C. & Karlin, A. Agonist binding site of Torpedo electric tissue nicotinic acetylcholine receptor. A negatively charged region of the delta subunit within 0.9 nm of the alpha subunit binding site disulfide. J Biol Chem **266**, 22603-12 (1991).
6. Czajkowski, C. & Karlin, A. Structure of the nicotinic receptor acetylcholine-binding site. Identification of acidic residues in the delta subunit within 0.9 nm of the 5 alpha subunit-binding. J Biol Chem **270**, 3160-4 (1995).
7. Czajkowski, C., Kaufmann, C. & Karlin, A. Negatively charged amino acid residues in the nicotinic receptor delta subunit that contribute to the binding of acetylcholine. Proc Natl Acad Sci U S A **90**, 6285-9 (1993).
8. Brejc, K. et al. Crystal structure of an ACh-binding protein reveals the ligand-binding domain of nicotinic receptors. Nature **411**, 269-76 (2001).
9. Miyazawa, A., Fujiyoshi, Y., Stowell, M. & Unwin, N. Nicotinic acetylcholine receptor at 4.6 A resolution: transverse tunnels in the channel wall. J Mol Biol **288**, 765-86 (1999).
10. Unwin, N. Refined structure of the nicotinic acetylcholine receptor at 4 angstrom resolution. Journal of Molecular Biology **346**, 967-989 (2005).
11. Akk, G., Zhou, M. & Auerbach, A. A mutational analysis of the acetylcholine receptor channel transmitter binding site. Biophys J **76**, 207-18 (1999).
12. Sine, S.M. et al. Naturally occurring mutations at the acetylcholine receptor binding site independently alter ACh binding and channel gating. J Gen Physiol **120**, 483-96 (2002).
13. Sixma, T.K. & Smit, A.B. Acetylcholine binding protein (AChBP): a secreted glial protein that provides a high-resolution model for the extracellular domain of pentameric ligand-gated ion channels. Annu Rev Biophys Biomol Struct **32**, 311-34 (2003).
14. Shi, J., Koeppe, J.R., Komives, E.A. & Taylor, P. Ligand-induced conformational changes in the acetylcholine-binding protein analyzed by hydrogen-deuterium exchange mass spectrometry. J Biol Chem **281**, 12170-7 (2006).
15. Hansen, S.B. et al. Structures of Aplysia AChBP complexes with nicotinic agonists and antagonists reveal distinctive binding interfaces and conformations. EMBO J **24**, 3635-46 (2005).
16. Hibbs, R.E., Radic, Z., Taylor, P. & Johnson, D.A. Influence of agonists and antagonists on the segmental motion of residues near the agonist binding pocket of the acetylcholine-binding protein. J Biol Chem **281**, 39708-18 (2006).
17. England, P.M., Zhang, Y., Dougherty, D.A. & Lester, H.A. Backbone mutations in transmembrane domains of a ligand-gated ion channel: implications for the mechanism of gating. Cell **96**, 89-98 (1999).
18. Cashin, A.L., Torrice, M.M., McMenimen, K.A., Lester, H.A. & Dougherty, D.A. Chemical-scale studies on the role of a conserved aspartate in preorganizing the agonist binding site of the nicotinic acetylcholine receptor. Biochemistry **46**, 630-9 (2007).

19. Martin, M., Czajkowski, C. & Karlin, A. The contributions of aspartyl residues in the acetylcholine receptor gamma and delta subunits to the binding of agonists and competitive antagonists. J Biol Chem **271**, 13497-503 (1996).
20. Martin, M.D. & Karlin, A. Functional effects on the acetylcholine receptor of multiple mutations of gamma Asp174 and delta Asp180. Biochemistry **36**, 10742-50 (1997).
21. Kash, T.L., Jenkins, A., Kelley, J.C., Trudell, J.R. & Harrison, N.L. Coupling of agonist binding to channel gating in the GABA(A) receptor. Nature **421**, 272-5 (2003).
22. Price, K.L., Millen, K.S. & Lummis, S.C. Transducing agonist binding to channel gating involves different interactions in 5-HT3 and GABAC receptors. J Biol Chem **282**, 25623-30 (2007).
23. Venkatachalan, S.P. & Czajkowski, C. A conserved salt bridge critical for GABAA receptor function and loop C dynamics. Proc Natl Acad Sci U S A (2008).
24. Eisenberg, D. & McLachlan, A.D. Solvation energy in protein folding and binding. Nature **319**, 199-203 (1986).
25. Grosman, C., Zhou, M. & Auerbach, A. Mapping the conformational wave of acetylcholine receptor channel gating. Nature **403**, 773-6 (2000).
26. Pangborn, A.B., Giardello, M.A., Grubbs, R.H., Rosen, R.K. & Timmers, F.J. Safe and convenient procedure for solvent purification. Organometallics **15**, 1518-1520 (1996).
27. Still, W.C., Kahn, M. & Mitra, A. Rapid Chromatographic Technique for Preparative Separations with Moderate Resolution. Journal of Organic Chemistry **43**, 2923-2925 (1978).
28. England, P.M., Lester, H.A. & Dougherty, D.A. Incorporation of esters into proteins: Improved synthesis of hydroxyacyl tRNAs. Tetrahedron Letters **40**, 6189-6192 (1999).
29. Mu, T. in Division of Chemistry and Chemical Engineering 126 (California Institute of Technology, Pasadena, 2006).
30. Laganis, E.D. & Chenard, B.L. METAL SILANOLATES - ORGANIC SOLUBLE EQUIVALENTS FOR O-2. Tetrahedron Letters **25**, 5831-5834 (1984).
31. Nowak, M.W. et al. In vivo incorporation of unnatural amino acids into ion channels in a Xenopus oocyte expression system. Methods Enzymol **293**, 504-529 (1998).
32. Filatov, G.N. & White, M.M. The role of conserved leucines in the M2 domain of the acetylcholine receptor in channel gating. Mol Pharmacol **48**, 379-84 (1995).
33. Labarca, C. et al. Channel gating governed symmetrically by conserved leucine residues in the M2 domain of nicotinic receptors. Nature **376**, 514-6 (1995).
34. Rodriguez, E.A., Lester, H.A. & Dougherty, D.A. In vivo incorporation of multiple unnatural amino acids through nonsense and frameshift suppression. Proc Natl Acad Sci U S A **103**, 8650-5 (2006).